Behavior of Manganese in Welding Fume (I)†

Nobuya IWAMOTO*1, Norimasa UMESAKI*2, Masayoshi KAMAI*3, Minoru KOBAYASHI*4, Shinsuke TSUTSUMI*4, Masahiro TAGA*5 and Akihito KUME*6

Abstract

The fumes produced from various welding materials have been investigated by means of chemical analysis, X-ray diffraction, EXAFS and optical absorption measurements. The results obtained are summarized as follows:

(1) From chemical analysis of fumes, it is indicated that in the case of arc welding with covered electrode, MnO content in the fumes increases with increasing Mn metal in welding rod. The MnO content in the fumes produced from high manganese welding rods was also approached to about 40 wt.%. On the other hand, in the case of gas shield welding, MnO content in the fumes increases with increasing CO_2 shield gas or by the addition of O_2 gas.

(2) X-ray diffraction analysis showed that manganese phases in the fumes produced from arc welding with covered electrode were $MnFe_2O_4$ and $KnMO_2$, but that in the case of gas shield welding, any crystalline phase with Mn element did not appear.

(3) EXAFS and optical absorption measurements suggest that the valence of Mn ions in the fumes studied is Mn^{2+} and/or Mn^{3+}.

KEY WORDS: (Welding fume) (Manganese oxide) (Chemical analysis) (X-ray diffraction) (EXAFS) (Optical absorption)

1. Introduction

It is well known that the fume produced from welding materials usually used contains about 5~15 wt.% of manganese in terms of MnO. It is pointed out that the long-time welding work in the bad environment causes manganese damage to the human body. The damage by manganese, which has valencies from zero to seven, is said to differ according to its valence number. The manganese valence as well as content is an important factor to determine whether the damage is caused or not. However, details of manganese state in fume produced from welding process have remained equivocal.

Therefore, in this work presented here, we have analyzed the manganese state in the fumes produced from various welding materials by means of chemical analysis, X-ray diffraction, EXAFS (Extended X-ray Absorption Fine Structure) and optical absorption measurements. As materials of study, we chose the typical commercial coated electrodes, the welding rods for hard facing with high manganese content and the gas shield-type electrode.

2. Experimental

Tables 1 and **2** indicate the welding conditions used and the chemical composition of the welding fumes produced, respectively, Fumes I-1~5 (ilmenite type) and L-1~3 (lime type) arose from trial product of electrode, while S-1 (lime-titania type) and H-1~2 (lime type) arose from commercial product.

In order to obtain the standard samples of manganese oxides such as MnO, Mn_3O_4, Mn_2O_3 and MnO_2, the analytical reagent grade Mn_3O_4 powder was used as a

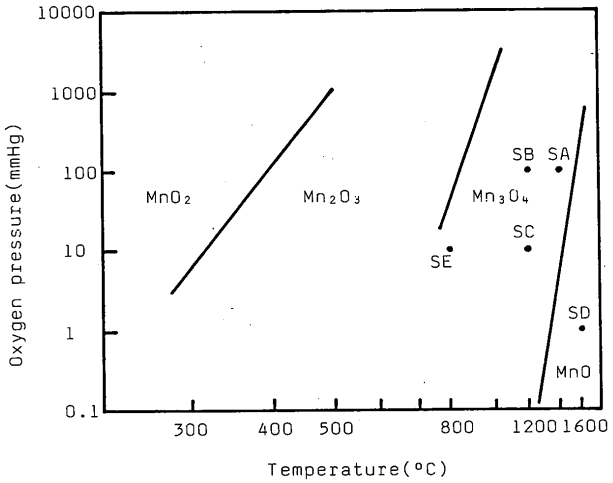

Fig. 1 Temperature vs. oxygen pressure diagram of manganese oxides.[1] The sintering conditions for standard samples SA~SE are plotted in this diagram.

† Received on April 30, 1984
*1 Professor
*2 Research Instructor
*3 Technical Assistant
*4 Kobe Steel, Ltd.
*5 Nippon Seisen Co., Ltd.
*6 Sumikin Welding Co., Ltd.

Transactions of JWRI is published by Welding Research Institute of Osaka University, Ibaraki, Osaka 567, Japan

Table 1 Welding materials and conditions.

Welding Method	Fume Sample	Used Steel	Welding Materials				Welding Conditions	
			Covering Type	Core Wire	Mn Content and Form in Welding Flux	Water Glass	Current	Shield Gas
Arc Welding with Covered Electrode	I-1	Mild Steel	Ilmenite	Mn less	Fe-Mn 15%	Na-K	230A	———
	I-2				Fe-Mn 15%	Na-K	230A	
	I-3			JIS SWY11	Fe-Mn 30%	Na-K	230A	
	I-4				MnO_2 24%	Na-K	230A	
	I-5				———	Na-K	230A	
	L-1	HT50	Lime	JIS SWY11	Fe-Mn 5%	Na-K	230A	———
	L-2				Fe-Mn 15%	Na-K	230A	
	L-3				Fe-Mn 15%	Na	230A	
	S-1	SUS	Lime-Titania	19Cr-9Ni-4Mn-1Mo			140A	———
	H-1	Hard Facing	Lime	16Mn-16Cr			170A	———
	H-2			13Mn			230A	
Gas Shielded Arc Welding	G-1	Mild Steel .HT50	JIS YCW2	———			300A	Ar
	G-2							80Ar-20CO_2
	G-3							50Ar-50CO_2
	G-4							CO_2
	G-5							98Ar-2O_2

Table 2 Chemical composition of welding fumes produced.

Fume Sample	Chemical Composition (wt.%)											
	Fe_2O_3	SiO_2	MnO	Sol.MnO	TiO_2	CaO	MgO	BaO	Cr_2O_3	Na_2O	K_2O	F
I-1	40.03	22.30	8.80	0.04	2.20	1.17	0.47	——	——	9.65	8.89	——
I-2	44.68	22.30	9.48	0.08	2.39	0.93	0.47	——	——	8.60	7.53	——
I-3	47.90	15.10	17.62	0.14	1.72	0.70	0.33	——	——	7.25	6.02	——
I-4	40.94	22.50	6.73	0.03	2.15	1.02	0.39	——	——	9.62	9.71	——
I-5	45.75	29.68	1.78	0.02	2.15	0.93	0.47	——	——	8.68	7.53	——
L-1	19.13	7.50	7.06	0.01	0.03	14.71	0.79	4.09	——	8.43	17.77	15.70
L-2	14.74	5.90	14.12	<0.01	0.03	13.47	0.73	3.77	——	8.63	17.64	15.72
L-3	16.36	6.80	16.10	0.06	0.03	14.05	0.68	4.19	——	18.37	5.58	14.77
S-1	9.38	6.30	15.15	0.24	6.63	3.41	0.10	——	6.47	0.51	32.68	14.04
H-1	12.95	3.80	38.86	0.09	0.04	7.54	0.08	——	4.38	7.16	11.00	11.50
H-2	30.38	2.80	26.33	<0.01	1.33	5.70	0.03	——	——	4.56	15.36	8.53
G-1	94.91	3.40	8.72	0.04	——	——	——	——	——	——	——	——
G-2	84.17	7.50	11.87	0.21	——	——	——	——	——	——	——	——
G-3	84.44	7.60	12.11	0.19	——	——	——	——	——	——	——	——
G-4	79.10	10.70	14.16	0.20	——	——	——	——	——	——	——	——
G-5	86.05	6.90	11.52	0.12	——	——	——	——	——	——	——	——

starting material. The powder of 1 g was dry-pressed into disk with 8 mmϕ under the pressure of 450 kg/cm^2. After forming, the disk was sintered by the experimental conditions given in **Table 3**. As shown in **Fig. 1**, these sintering conditions studied were plotted in the temperature vs. oxygen pressure diagram of manganese oxides[1].

X-ray diffraction experiment was carried out with the use of Rigaku RAD-rA diffractometer and RU200 12 kW rotating anode generator. The Cu Kα radiation (voltage: 50 kV and current: 180 mA) monochromatized by a curved graphite crystal was used. A slit system of 1° (DS: divergence slit) and 0.3 mm (RS: receiving slit) was employed.

Table 3 Sintering conditions of standard samples.

Sample	Sintering Temp. (°C)	Oxygen Pressure
SA	1400	100/760
SB	1200	100/760
SC	1200	10/760
SD	1600	1/760
SE	800	10/760

EXAFS (Extended X-ray Absorption Fine Structure) spectra of Mn atom (K-absorption edge energy: 6564 eV)

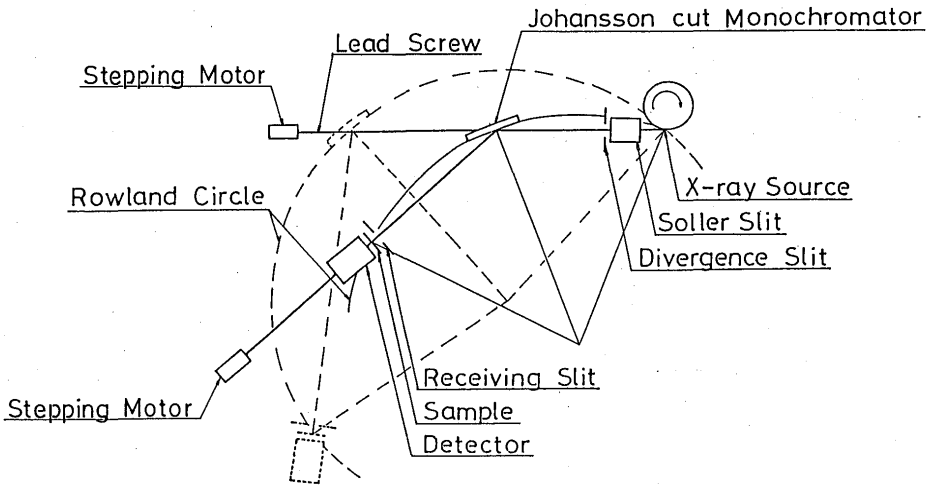

Fig. 2 Schematic diagram of focusing EXAFS system used.

in the welding fumes and the standard samples were measured with a Rigaku EXAFS spectrometer with a Johansson-type LiF crystal. A schematic diagram of the focusing EXAFS system used in shown in **Fig. 2.** The X-ray radiation (voltage: 20 kV and current: 100 mA) was generated by a Rigaku RU200 12 kW rotating anode source. A slit system of 2° (DS) and 0.2 mm (RS) was employed. The specimens for EXAFS measurement were prepared as films in the same manner as White and Mckinstry.[2] The X-ray intensities were measured in the energy range from 6400 to 7000 eV at 6 eV intervals by a scintillation counter. The absorption coefficient μx is given by the following equation,

$$\mu x = \ln(I_0/I), \qquad (1)$$

where x is the specimen thickness, and I_0 and I are intensities of the incident and transmitted X-ray beams, respectively.

Optical absorption measurement was performed with the use of Hitachi 323 double-beam recording spectrometer.

3. Results and Discussion

3.1 Chemical Analysis

As shown in Table 2, in the case of the welding fluxes of ilmenite type and/or lime type for HT50, MnO content in the welding fumes (I-1~3 and L-1~3) increases with increasing Fe-Mn content in the welding fluxes. It is, however, recognized that MnO content in the fumes (I-4 and I-5) produced from the MnO_2 welding flux was reduced to one-third of its MnO value of the fumes (I-1~3 and L-1~3) produced from Fe-Mn welding fluxes. It is possible to show that the amount of MnO in the fume (S-1) was about 15 wt.% when the stainless steel was used for electrode, and that the MnO content in the fumes (H-1 and H-2) produced from hard facing was about 25~40 wt.%. In the case of the gas shield arc welding used with Ar-CO_2 shield gas, it is recognized from Table 2 that MnO content in the fumes (G-1~5) increases with increasing CO_2 shield gas or by the addition of O_2 gas. The greatest amount of solbule MnO in the fumes was 0.24 wt.%.

3.2 X-ray Diffraction Analysis

Fig. 3 shows the typical X-ray diffraction patterns in the welding fumes studied. The obtained results indicate that all of the fumes contain Fe_3O_4, and that metal Fe exists in the fumes (G-1~5) produced from the gas shield arc welding. The fumes with MnO>6 wt.% (I-1~4, L-1~3, S-1 and H-1~2), which was produced from arc welding with covered electrode, had $MnFe_2O_4$ and $KMnO_2$ (or $K_2Mn_4O_8$), while there was no $KMnO_2$ (or $K_2Mn_4O_8$) in the fume (S-1) used with stainless steel. Also, in the case of the fumes (G-1~5) produced from gas shield welding, the amount of MnO and Fe_3O_4 were 8~15 wt.% and 80~95 wt.%, respectively. Consequently, any crystalline phase with Mn element did not appear. Fulorides such as NaF, CaF_2 and $KCaF_3$ existing in the fumes (L-1~3 and H-1~2) arose from lime type fluxes used with HT50 and/or hard facing. The crystalline phase of Cr element in the fumes (S-1 and H-1) was K_2CrO_4.

From the X-ray diffraction analysis, the crystalline phases of Mn element in the fumes studied were $MnFe_2O_4$ and $KMnO_2$ (or $K_2Mn_4O_8$). Therefore, it is concluded that the valence of Mn ions in the fumes is Mn^{2+} and/or Mn^{3+}.

3.3 EXAFS Analysis

As an example, **Fig. 4** shows an EXAFS spectrum of

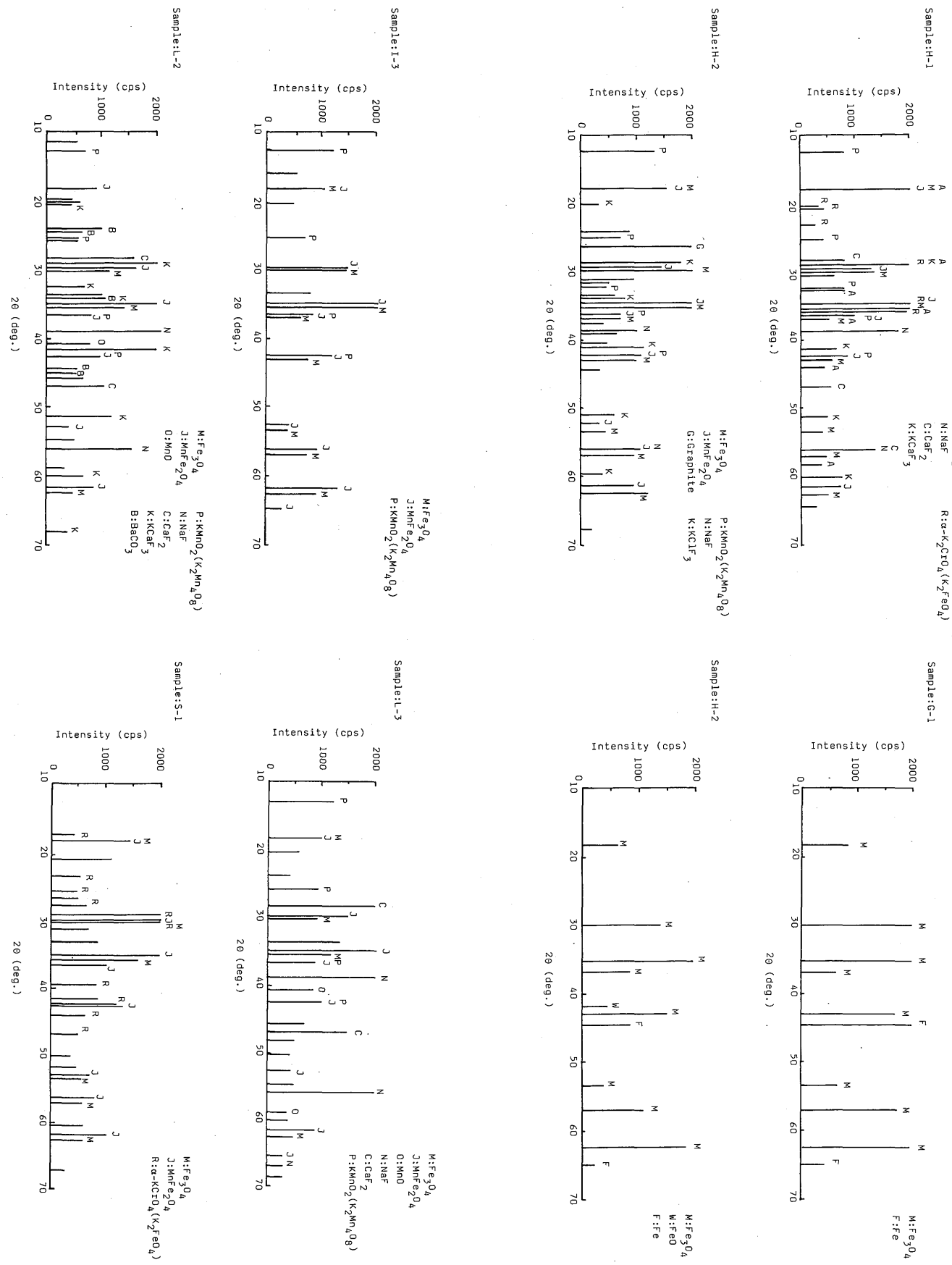

Fig. 3 X-ray diffraction patterns of typical welding fumes.

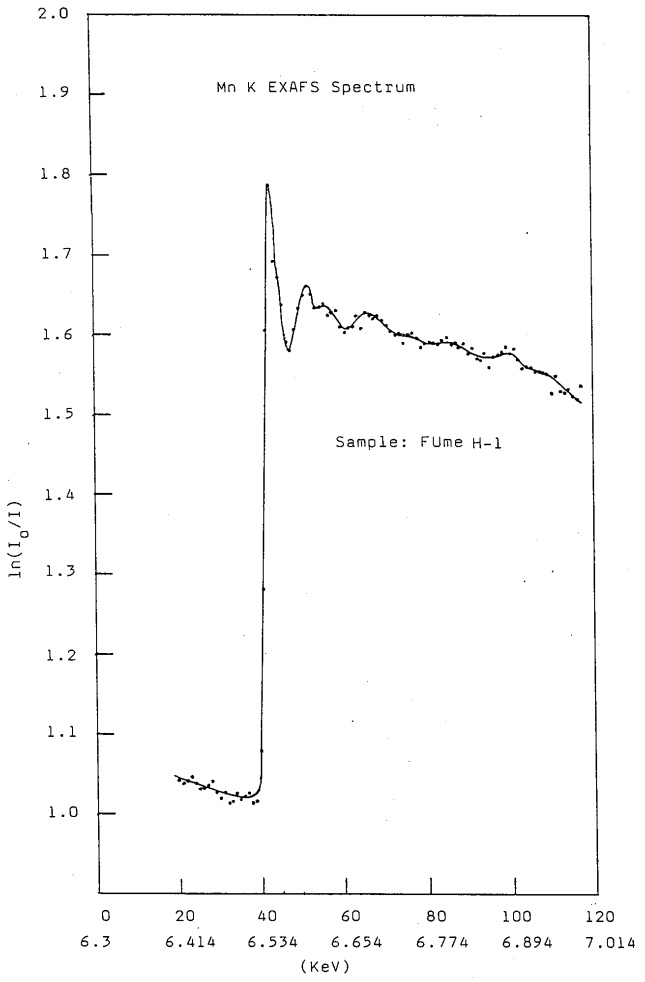

Fig. 4 EXAFS spectrum of welding fume H-1.

the H-1 fume. **Fig. 5** indicates the typical X-ray absorption spectrum for all the oxides[2] and makes the somewhat arbitray distribution between X-ray absorption near edge structure (XANES) and EXAFS. As shown in this figure, EXAFS refers to the oscillatory variation behavior of the X-ray absorption as a function of photon energy. Such oscillations can extend up to 1000 eV above the K-absorption edge energy. Point A is the energy of the initial increase in absorption measured at the point of intersection of a line through the background and a line

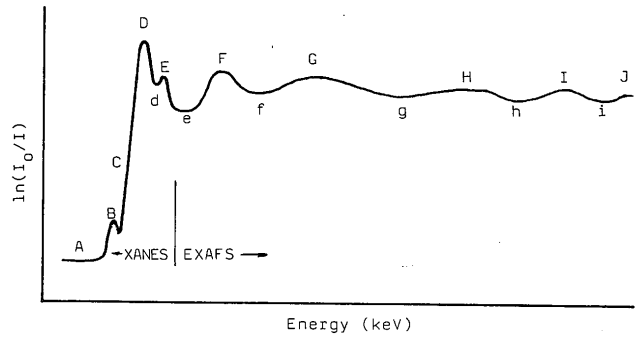

Fig. 5 Schematic absorption curve.

tangent to the slope of the edge. Point B corresponds to the energy of a small absorption maximum that is often absent. Point C indicates the position of the edge at one-half height. Point D usually corresponds to the energy of the first major absorption peak. It is often assumed to correspond to the energy of the transition 1s → 4s. Point E, when present, is usually the second resolved maximum, possibly corresponding to the energy at which a 1s electron escapes the energy-level system of the "ionized atom". Maxima beyond point F are sequentially labelled with capital letters as indicated in Fig. 5. **Fig. 6** shows the energies of absorption features of the fumes H-1 and H-2 having set Point A equal to zero, and is compared with the

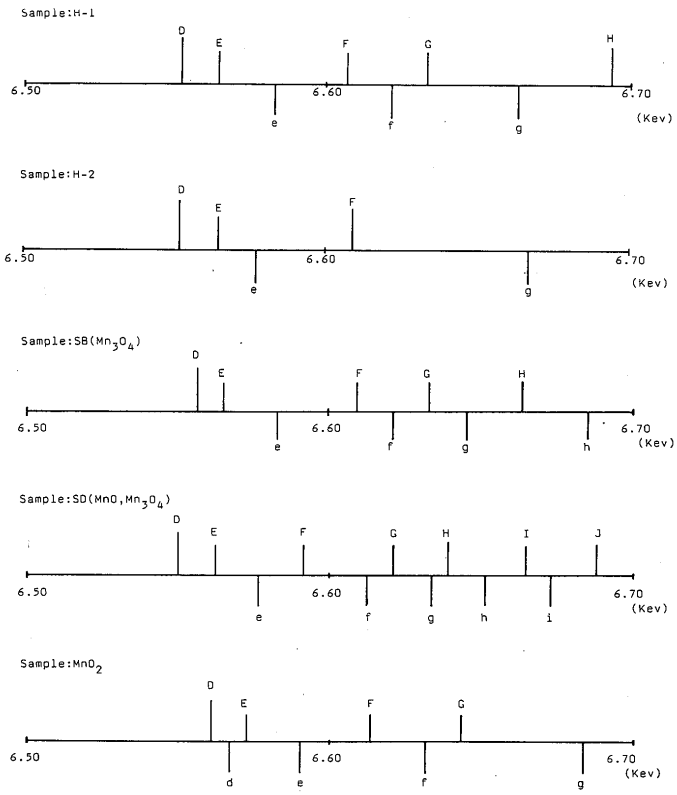

Fig. 6 Energies of EXAFS between welding fumes and standard samples.

energies of these fumes and the standard samples MnO_2, SB (Mn_3O_4) and SD ($MnO + Mn_3O_4$). As shown in this figure, the energies of absorption structure obtained from the fumes H-1 and H-2 were good agreement with those of the manganese oxides MnO and Mn_3O_4. These obtained results appear that the valence of Mn ions in these fumes is Mn^{2+} and/or Mn^{3+}. Unfortunately, from the qualitative EXAFS data, we could not determine wether Mn^{4+} ions existing in the two fumes or not.

3.4 Optical Absorption Analysis

Figures 7 and 8 show the optical absorption spectra of

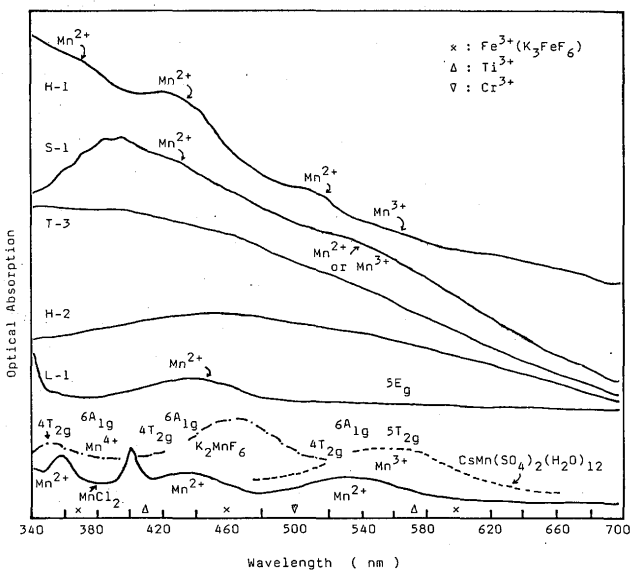

Fig. 7 Optical absorption spectra of welding fumes.

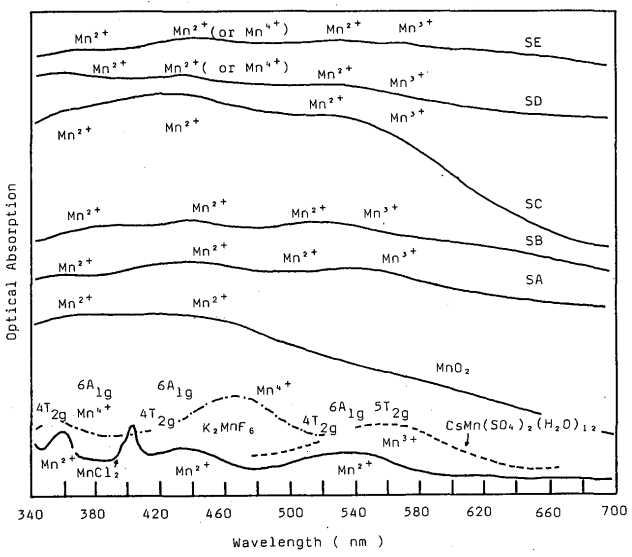

Fig. 8 Optical absorption spectra of standard samples.

the Fumes H-1~2, L-1, S-1 and T-1 and the standard samples SA, SC, SD, SE, $MnCl_2$,[3] K_2MnF_6[4] and $CsMn(SO_4)_2(H_2O)_{12}$,[5,6] respectively. As shown in this figure, the existence of Mn^{2+} and Mn^{3+} ions was confirmed for both the fumes and the standard samples. Mn^{4+} ions gives an absorption peak at near 460 nm, but the absorption peak due to Mn^{2+} ions also appears in this region. Therefore, it is considered to be difficult to discuss the existence of Mn^{4+} ions in the fumes from the optical absorption measurement.

4. Conclusion

The investigation of fumes produced from various welding materials have been carried out. The results obtained are as follows:

(1) From chemical analysis of fumes, it is indicated that in the case of arc welding with covered electrode, MnO content in the fumes increases with increasing Mn metal in welding rod. The MnO content in the fumes produced from high manganese welding rods was also approched to about 40 wt.%. On the other hand, in the case of gas shield welding, MnO content in the fumes increases with increasing CO_2 shield gas or by the addition of O_2 gas.

(2) X-ray diffraction analysis showed that manganese phases in the fumes produced from arc welding with covered electrode were $MnFe_2O_4$ and $KnMO_2$, but that in the case of gas shield welding, any crystalline phase with Mn element did not appear.

(3) EXAFS and optical absorption measurements suggest that the valence of Mn ions in the fumes studied is Mn^{2+} and/or Mn^{3+}.

References

1) P.R.S. Jackson and G.R. Wallwork: High Temperature Technology, **1** (1983) 259.

2) E.W. White and H.A. Mckinstry: Advances in X-ray Analysis, edited by G.R. Mallet, M. Fay and W.M. Mveller, Vol. **9** (1966), p.376~392, Plenum Press, New York.

3) C.K. Jφrgensen: Acta Chem. Scand., 8 (1954), 1502.

4) C.K. Jφrgensen: Acta Chem. Scand., **12** (1958), 1539.

5) R.S. Drago, D.W. Meek and R, Longhi: Inorg. Chem., **2** (1963).

6) A.B.P. Lever: Inorganic Electronic Spectroscopy, Chapter 9, (1968), Elsevier Publishing Co., Amsterdam.